

Time development of photon statistics in fluorescence from single atoms

T. W. Hodapp

Physics Department, Hamline University, St. Paul, Minnesota 55104

M. A. Finn* and G. W. Greenlees

School of Physics and Astronomy, University of Minnesota, Minneapolis, Minnesota 55455

(Received 28 February 1992)

Photons spontaneously emitted from single atoms are necessarily antibunched in time. The statistics of the photon time record, however, can show sub-Poissonian or even super-Poissonian statistics and depend strongly on the time interval used for analysis. In this work we have analyzed photon arrival times from resonantly excited barium atoms in an atomic beam observed under single-atom conditions. The time-interval dependence of photon statistics is presented, showing the connection between antibunching and sub-Poissonian statistics (at times comparable to the spontaneous-decay lifetime of the atom) as well as the evolution of the statistics in the long-time limit.

PACS number(s): 42.50.Dv, 42.50.Ar, 32.80.-t

I. INTRODUCTION

The distinctly quantum-mechanical behavior of the interaction between light and atoms has been brought out in recent years by a number of experiments in the field of quantum optics. The discrete nature of transitions between atomic energy states was demonstrated graphically by observations of quantum jumps both directly [1-3] and indirectly [4]. A consequence of these discrete jumps for an atom is a time gap in the spontaneously emitted photon emission time sequence. This gap between photons, known as antibunching, has been observed in a number of experiments [3,5-7] and can give rise to non-classical statistics of the emitted light. In experiments on single atoms, observations have been made of the photon statistics for time intervals considerably longer than the natural-decay lifetime of the atom. In this regime the statistics approach their steady-state values.

For a counting time interval t , the probability distribution $p(n)$ (where n is the photon number) can be described by a parameter Q , originally introduced by Mandel [8],

$$Q = \frac{\langle n^{(2)} \rangle - \langle n \rangle^2}{\langle n \rangle}, \quad (1)$$

and relates the first $\langle n \rangle$ and second $\langle n^{(2)} \rangle$ factorial moments of the distribution. Sub-Poissonian ($Q < 0$) statistics have been observed by a number of groups [9-15], and recently Poissonian ($Q = 0$) and super-Poissonian ($Q > 0$) statistics have been reported [13-15]. The experimental results have agreed well with the theoretical models set forth by Mandel [8], Cook [16], and others [17,18]. No investigations have been made to date, however, to the authors' knowledge, into the statistical nature of spontaneously emitted light for time intervals short compared to the natural-decay lifetime τ of the atom. The behavior of light in this time regime can show the devel-

opment of the statistics of emitted photons and a clear relationship between antibunching and photon statistics (confusion on this point has been discussed recently in the literature [19]).

In this article we present experimental results relating the time development of photon statistics for resonant and near-resonant fluorescence of individual barium atoms in an atomic beam. In this experiment, data were recorded in such a way as to make possible time-resolved studies of the photon statistics.

II. THEORETICAL CONSIDERATIONS

To demonstrate the connection between antibunching and the statistical nature of atomic fluorescence, it is useful to evaluate Q as a function of time. At large counting times $t \gg \tau$, Cook [16] showed that Q has the form

$$Q = \frac{(-I/I_0)(3-D^2)}{[1+I/I_0+D^2]^2}, \quad (2)$$

where I/I_0 and D are, respectively, dimensionless intensity and detuning parameters given by

$$I/I_0 = \frac{\Omega^2}{2\beta^2}, \quad (3)$$

$$D = 2\tau(\omega - \omega_0). \quad (4)$$

Here ω_0 and ω are the frequencies of the atomic transition and the laser field, Ω is the Rabi frequency, and $\beta = (2\tau)^{-1}$ is half the Einstein A coefficient.

It can be seen from Eq. (2) that Q is negative for all values of I/I_0 and zero detuning (resonance conditions) and becomes positive at sufficiently large detunings. What is not indicated is that for all values of detuning and power, at short times (of order τ), Q is negative. This

behavior is a consequence of the antibunched nature of the light.

To find an expression for Q as a function of time we start with an expression from Mandel [8] of the first two factorial moments of the photon-number distribution in terms of the two-time intensity correlation function $g^{(2)}(t)$;

$$\langle n^{(2)} \rangle = \langle I \rangle^2 2! \int_0^T dt_2 \int_0^{t_2} dt g^{(2)}(t), \quad (5)$$

$$\langle n^{(1)} \rangle = \langle I \rangle T, \quad (6)$$

where T is the measurement time, and $\langle I \rangle$ is the steady-state fluorescence intensity given by

$$\langle I \rangle = \frac{1}{2\tau} \left[\frac{I/I_0}{1 + I/I_0 + D^2} \right]. \quad (7)$$

The two-time intensity correlation function can be found in a fully quantized treatment of the interaction between a two-level atom and the electromagnetic field. This subject has been studied by several workers [20], and it has been shown that the correlation between two photons, the first having been emitted at $t=0$ and the second at τ , is given by

$$g^{(2)}(\tau) = 1 + Ke^{L\tau} + Me^{N\tau} [P \cos(R\tau) + S \sin(R\tau)], \quad (8)$$

where

$$Q(t) = -\langle I \rangle \left[\frac{MPN - MRS}{N^2 + R^2} + \frac{K}{L} \right] - \frac{2\langle I \rangle K}{tL^2} [1 - e^{Lt}] + \frac{2\langle I \rangle M}{(N^2 + R^2)^2 t} [e^{Nt} \{ (PN^2 - PR^2 - 2RSN) \cos(Rt) + (SN^2 - SR^2 - 2RPN) \sin(Rt) \} - (PN^2 - PR^2 - 2RSN)]. \quad (11)$$

This function is negative for times short compared to τ , and reduces to Eq. (2) for long times ($t \gg \tau$).

III. EXPERIMENT

In this experiment, the $6s^2 1S_0 \rightarrow 6s6p^1P_1$ transition at 554 nm of neutral ^{138}Ba ($\tau = 8.37$ nsec [21]) was resonantly and near-resonantly excited by light from a narrow-band laser. A high-efficiency light-collection system recorded individual photon arrival times as each atom passed through the laser field. In this way, the statistics of the photon record were available to be analyzed for

$$K = - \frac{\beta(A + \frac{1}{3})(\frac{1}{9} - \frac{4}{3}A + 4A^2 + D^2)}{2\langle I \rangle(\frac{1}{2}A - \frac{1}{3})(B^2 + 9A^2)},$$

$$L = (-\frac{4}{3} + 2A)\beta,$$

$$M = -\frac{2\beta}{\langle I \rangle},$$

$$N = -(\frac{4}{3} + A)\beta, \quad (9)$$

$$P = \frac{FH + GJ}{H^2 + J^2},$$

$$R = B\beta,$$

$$S = \frac{FJ - GH}{H^2 + J^2}$$

are expressed in terms of

$$A = \frac{1}{2}(\eta_+ + \eta_-),$$

$$B = \frac{\sqrt{3}}{2}(\eta_+ - \eta_-),$$

$$\eta_{\pm} = \frac{1}{3} \{ 9I/I_0 - 9D^2 - 1 \pm [(9I/I_0 - 9D^2 - 1)^2 + (6I/I_0 + 3D^2 - 1)^3]^{1/2} \}^{1/3}, \quad (10)$$

$$F = \frac{2}{27} + \frac{1}{3}A + \frac{2}{3}D^2 - AD^2 - A^3 + 3AB^2,$$

$$G = -\frac{1}{3}B + BD^2 - B^3 + 3A^2B,$$

$$H = 8AB^2 + \frac{8}{3}B^2,$$

$$J = 8AB + 6A^2B - 2B^3.$$

To evaluate Q , Eqs. (1), (5), and (8) are combined and the integral evaluated. This yields

various counting intervals, making possible a time-dependent evaluation of Q .

The details of this experiment have been described previously [13], consequently, only the essential aspects are described here. The laser light was generated by a narrowed (~ 1 MHz linewidth), tunable single-mode dye laser (Spectra Physics 380D), which was frequency locked to a transmission fringe of a 470-MHz free spectral range confocal Fabry-Pérot étalon. A separate transmission fringe from a stabilized 633-nm HeNe laser (Laboratory for Science 220) provided a signal to lock the étalon's length. The HeNe laser was tunable over a limited range in discrete 600-kHz steps. By tuning the HeNe, the

étalon's length was changed, pulling the dye laser's frequency with it. This allowed a limited but extremely stable tuning of the dye laser (< 1 MHz/h). The dye laser light was imaged into a rectangular spot (4.9×1.4 mm²) aligned along the path of a highly collimated, tenuous atomic beam (~ 250 atoms/sec). This orthogonal intersection occurred at the line focus of two back-to-back polished elliptical cylinders. Approximately 48% of the light emitted by the atoms was collected onto a pair of high quantum efficiency photomultipliers (EMI 9658RA) placed at the conjugate foci of the cylinders. Signals from the two photomultipliers (PMT's) were fed into a pair of time digitizers (LeCroy 2228A Mod 203) and recorded via computer control.

To determine the presence of an atom in the laser field and to discriminate against background events, a hardware coincidence circuit was employed. This circuit divided the time following an initial photon signal into three sequential intervals *A* ($3 \mu\text{sec}$), *B* ($5 \mu\text{sec}$), and *C* ($5 \mu\text{sec}$). To register a valid event, the circuit required a photon from each of the two PMT's during both *A* and *C* periods. If this requirement was met, data from the *B* period were recorded. This ensured that events were rejected if fluorescence from a barium atom was interrupted in any way, either by an atom leaving the laser field prematurely or by an atom's decay to one of a set of metastable *D* states (branching ratio 1:280 [22]). This was essential as lifetimes of the *D* states are considerably longer than the atom's transit time through the detector.

Data were taken for a variety of detunings from $D=0 \rightarrow 2.1$ ($\Delta\omega/2\pi=0 \rightarrow 19.9$ MHz). For off-resonant

detunings, frequencies were chosen on the low-energy side of the ¹³⁸Ba transition to avoid interference from resonance peaks of other stable isotopes of barium. To keep data recording rates at a reasonable value ($\sim 10/\text{sec}$) as well as to simplify corrections to the data, the laser intensity was set for each detuning so that the measured fluorescence rate was constant throughout all runs. During each run, light from 200 000 individual atoms was recorded over the course of a 5–10-h period. Throughout a run, the intensity of the dye laser was monitored and maintained within $\sim 5\%$ of the original value.

IV. ANALYSIS AND RESULTS

Analysis of the recorded photon arrival times proceeded in two stages. First, the two records (one from each PMT) were merged by accepting valid photon events from one PMT, and then the other. This technique, in which alternate photons are recorded from each of the two photomultipliers, was necessary as instrumentation dead time and afterpulsing effects from the phototubes distorted the data. A complete analysis of this technique has been published previously [23]. The second stage was to compile a probability distribution for the desired measurement interval. The complete photon time record was split into intervals ranging from 5 to 100 nsec and the statistics evaluated. Shorter time periods yielded an increased number of intervals, consequently, the statistical errors for these points were smaller.

A number of corrections were applied to the data including effects of multiple atoms in the laser field; events

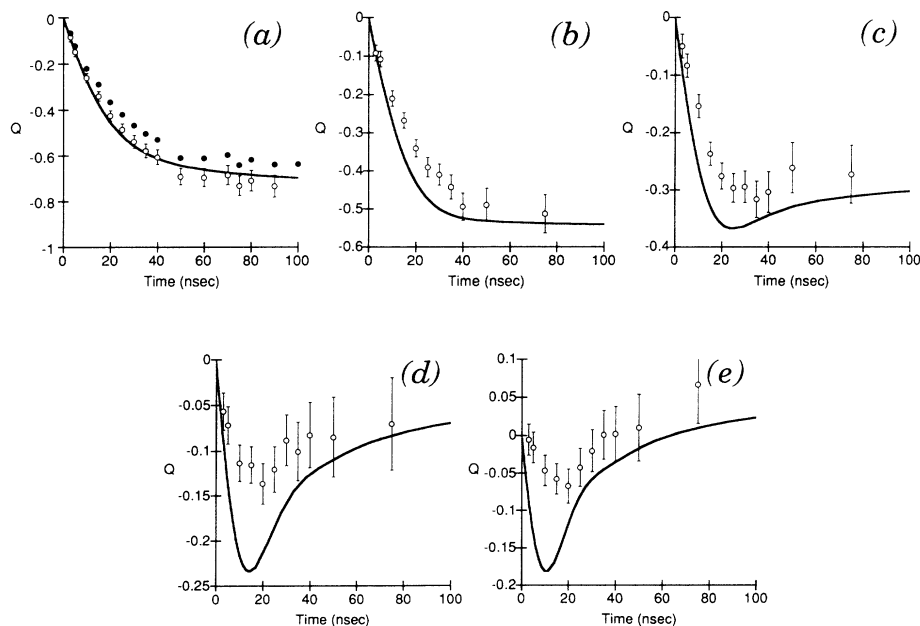


FIG. 1. Experimental and theoretical values for Q as a function of measurement interval for five different detunings D ($\Delta\omega/2\pi$) and dimensionless intensities (I/I_0): (a) $D=0.0$ (0 MHz), $I/I_0=0.97$; (b) $D=0.50$ (4.8 MHz), $I/I_0=1.26$; (c) $D=0.96$ (9.1 MHz), $I/I_0=2.00$; (d) $D=1.61$ (15.3 MHz), $I/I_0=3.50$; (e) $D=2.09$ (19.9 MHz), $I/I_0=5.19$. In each case error bars represent statistical uncertainties ($\sqrt{2/N}$). (a) also includes data points corrected only for collection efficiency (filled circles) to show the magnitude of corrections made to the data.

triggered by background counts; background contamination; laser frequency and intensity variation over the course of a run; second-order dead-time effects, and the collection efficiency of the apparatus. A complete description of each of these corrections is given in Ref. [24] and we present here only an outline of how each correction was determined.

The coincidence circuit used was modeled via computer to determine the fraction of events which contained more than a single atom ($\sim 0.35\%$) or events in which background counts initiated and fulfilled a trigger ($0.36\text{--}0.80\%$). Corrections due to both background triggers and multiple atoms were calculated by convoluting together probability distributions for zero, one, and two atoms present in the laser beam. Background contamination of single-atom events was estimated as well in this way by incorporating the measured background count rate ($1.5\text{--}5.0$ kHz per photomultiplier). These calculations agreed with observed event rates both with and without atoms present in the laser field.

Corrections due to laser intensity and frequency variation over the course of a run were estimated by evaluating the integrated change in theoretical values of Q over the range of parameters measured throughout each individual data run.

The dead time of photomultipliers and their associated electronics was overcome to first order by ensuring that successive photons were only used from alternate photomultipliers. If, however, two photons (one from each tube) occurred in close temporal proximity, the initial tube might still be "dead" when it was again thought to be active. The effect of this second-order dead time on Q was estimated by evaluating Q from an incandescent (Poisson) light source running at an intensity equivalent to that given off by a single atom (~ 270 kHz per photomultiplier).

The collection efficiency of the light collector was determined by measuring the fluorescent rate for a single atom [Eq. (7)] as a function of laser intensity. The resulting "saturation curve" provided a total collection efficiency parameter ($\eta=0.018$) which was in good agreement with direct measurements of the light-collection geometry and photomultiplier sensitivities.

Each of the corrections except the collection efficiency were small compared to the statistical error (for N measurements $\Delta Q = \sqrt{2/N}$). The correction due to the collection efficiency affected Q in a straightforward manner [25], as measured Q scales linearly with η , $Q_{\text{meas}} = \frac{1}{2}\eta Q$. The factor of 2 is due to the reduction in collection efficiency imposed by the alternating technique.

Plots for each detuning are given in Fig. 1. The experimental data (with statistical errors) and theory from Eq. (11) are plotted for each of the five intensity and detuning conditions measured. The first graph [Fig. 1(a)] includes raw data, corrected only for collection efficiency (solid circles), as well as corrected points (open circles) to show magnitudes of corrections made to the final data. Each graph is characterized by sub-Poissonian statistics at short times even though their asymptotic values are, in most cases, quite different. A good qualitative agreement between theory and data is seen. However, for short

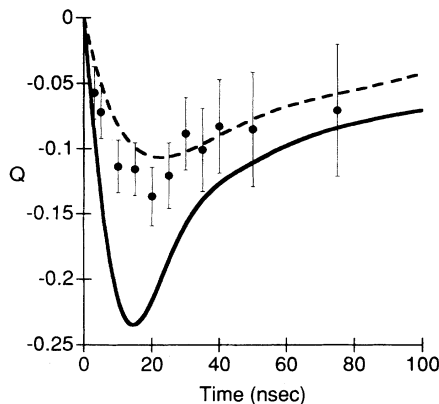


FIG. 2. Results of a Monte Carlo simulation with an added time jitter of 22 nsec FWHM are plotted as a dashed line for a detuning of $D=1.6$. Experimental data and theoretical values for this detuning are plotted again [as in Fig. 1(d)] to provide a comparison with the results of the simulation.

times ($t \approx \tau$) the data do not lie directly with the theory, rather they follow its trend. This characteristic is most obvious for the larger detuning cases. We have investigated this effect and attribute it to time jitter inherent to the particular PMT's we used. These photomultipliers were selected for high quantum efficiency and low dark current rather than for timing precision, consequently, information at short times was lost. The manufacturer's specification of the average time uncertainty for this tube was 22 nsec full width at half maximum (FWHM). Figure 2 shows the results of a Monte Carlo simulation for the $D=1.6$ detuning ($I/I_0=3.5$), with a Gaussian 22 nsec FWHM time jitter. The Monte Carlo adjustments to the theory are represented by the dashed line. The solid line represents the theory [as in Fig. 1(d)] and the filled circles represent data points for these detuning and power conditions. These conditions represent a worst case disagreement between theory and experiment. It can be seen, however, that the time-jittered theory provides an adequate explanation for the discrepancies between theory and experiment seen in Fig. 1. Monte Carlo simulations were tested for each of the conditions and good agreement was found throughout.

In conclusion, we have examined the temporal evolution of the statistical nature of light from single-atom resonant and near-resonant fluorescence. Good agreement in all cases was found between theoretical predictions and experimental data. The antibunched quality of the light is evident for short-time scales ($t \ll \tau$) and in all cases this gives sub-Poissonian statistics. These data show clearly how Poissonian or even super-Poissonian light in the limit of long measurement intervals can exhibit antibunching and a sub-Poissonian character at short times.

ACKNOWLEDGMENTS

The authors thank Travis Novotny for his help with the Monte Carlo simulations. This work was supported in part by the National Science Foundation and the Joyce Foundation.

*Present address: Clarus Medical Systems, Inc., 2605 Fernbrook Lane, Plymouth, MN 55447.

- [1] W. Nagourney, J. Sandberg, and H. Dehmelt, *Phys. Rev. Lett.* **56**, 2797 (1986).
- [2] Th. Sauter, W. Neuhauser, R. Blatt, and P. E. Toschek, *Phys. Rev. Lett.* **57**, 1696 (1986).
- [3] J. C. Bergquist, R. G. Hulet, W. M. Itano, and D. J. Wineland, *Phys. Rev. Lett.* **57**, 1699 (1986).
- [4] M. A. Finn, G. W. Greenlees, and D. A. Lewis, *Opt. Commun.* **60**, 149 (1986).
- [5] H. J. Kimble, M. Dagenais, and L. Mandel, *Phys. Rev. Lett.* **39**, 691 (1977).
- [6] M. Dagenais and L. Mandel, *Phys. Rev. A* **18**, 2217 (1978).
- [7] G. Rempe, R. J. Thompson, R. J. Brecha, W. D. Lee, and H. J. Kimble, *Phys. Rev. Lett.* **67**, 1727 (1991).
- [8] L. Mandel, *Opt. Lett.* **4**, 205 (1979).
- [9] R. Short and L. Mandel, *Phys. Rev. Lett.* **51**, 384 (1983).
- [10] F. Diedrich and H. Walther, *Phys. Rev. Lett.* **58**, 203 (1987).
- [11] W. M. Itano, J. C. Bergquist, and D. J. Wineland, *Phys. Rev. A* **38**, 559 (1988).
- [12] M. A. Finn, G. W. Greenlees, T. W. Hodapp, and D. A. Lewis, *Phys. Rev. A* **40**, 1704 (1989).
- [13] T. W. Hodapp, G. W. Greenlees, M. A. Finn, and D. A. Lewis, *Phys. Rev. A* **41**, 2698 (1990).
- [14] B. G. Oldaker, P. J. Martin, P. L. Gould, M. Xiao, and D. E. Pritchard, *Phys. Rev. Lett.* **65**, 1555 (1990).
- [15] M. D. Hoogerland, M. N. J. H. Wijnands, H. A. J. Senhorst, H. C. W. Beijerinck, and K. A. H. van Leeuwen, *Phys. Rev. Lett.* **65**, 1559 (1990).
- [16] R. J. Cook, *Phys. Rev. A* **22**, 1078 (1980).
- [17] S. Singh, *Opt. Commun.* **44**, 254 (1983).
- [18] H. F. Arnoldus and G. Nienhuis, *Opt. Acta* **30**, 1573 (1983).
- [19] X. T. Zou and L. Mandel, *Phys. Rev. A* **41**, 475 (1990).
- [20] See, for example, H. J. Kimble and L. Mandel, *Phys. Rev. A* **13**, 2123 (1976).
- [21] L. Jahreiss and M. C. E. Huber, *Phys. Rev. A* **31**, 692 (1985).
- [22] D. A. Lewis, J. Kumar, M. A. Finn, and G. W. Greenlees, *Phys. Rev. A* **35**, 131 (1987).
- [23] M. A. Finn, G. W. Greenlees, T. W. Hodapp, and D. A. Lewis, *Rev. Sci. Instrum.* **59**, 2457 (1988).
- [24] For a complete description of the corrections see T. W. Hodapp, Ph.D. thesis, University of Minnesota, 1988 (unpublished).
- [25] J. A. Abate, H. J. Kimble, and L. Mandel, *Phys. Rev. A* **14**, 788 (1976).